




Article

Optimizing Dynamic Evacuation Using Mixed-Integer Linear Programming

Hamoud Bin Obaid ¹, Theodore B. Trafalis ², Mastoor M. Abushaega ^{3,*}, Abdulhadi Altherwi ³
and Ahmed Hamzi ³

¹ Department of Industrial Engineering, King Saud University, Riyadh 11421, Saudi Arabia; hsbinoaid@ksu.edu.sa

² Department of Industrial and Systems Engineering, University of Oklahoma, 202 W Boyd St. Lab 28, Norman, OK 73019, USA; ttrafal@ou.edu

³ Department of Industrial Engineering, College of Engineering and Computer Science, Jazan University, Jazan 45142, Saudi Arabia; aaaltherwi@jazanu.edu.sa (A.A.); amhamzi@jazanu.edu.sa (A.H.)

* Correspondence: mabushaega@jazanu.edu.sa

Abstract: This study presents a new approach to optimize the dynamic evacuation process through a dynamic traffic assignment model formulated using mixed-integer linear programming (MILP). The model approximates the travel time for evacuee groups with a piecewise linear function that accounts for variations in travel time due to load-dependent factors. Significant delays are transferred to subsequent groups to simulate delay propagation. The primary objective is to minimize the network clearance time—the total time required for the last group of evacuees to reach safety from the start of the evacuation. Given the model's computational intensity, a simplified version is introduced for comparison. Both the original and simplified models are tested on small networks and benchmarked against the Cell Transmission Model, a well-regarded method in dynamic traffic assignment literature. Additional objectives, including average travel time and average evacuation time, are explored. A sensitivity analysis is conducted to assess how varying the number of evacuee groups impacts model outcomes.

Keywords: evacuation planning; disaster management; optimal routing; mixed-integer linear programming; dynamic traffic assignment

MSC: 90C11; 90B20; 90C29; 90B06; 90B10



Academic Editor: Amir Hossein Nobil

Received: 20 November 2024

Revised: 17 December 2024

Accepted: 23 December 2024

Published: 24 December 2024

Citation: Obaid, H.B.; Trafalis, T.B.; Abushaega, M.M.; Altherwi, A.; Hamzi, A. Optimizing Dynamic Evacuation Using Mixed-Integer Linear Programming. *Mathematics* **2025**, *13*, 12. <https://doi.org/10.3390/math13010012>

Copyright: © 2024 by the authors. Licensee MDPI, Basel, Switzerland. This article is an open access article distributed under the terms and conditions of the Creative Commons Attribution (CC BY) license (<https://creativecommons.org/licenses/by/4.0/>).

1. Introduction

Evacuation is essential in the case of natural and manmade disasters such as hurricanes, nuclear disasters, fire accidents, and terrorism epidemics. Random evacuation plans can increase risks and incur more losses. Hence, numerous simulation and mathematical models have been proposed over the past few decades to help transportation planners make decisions to reduce costs and protect lives. However, the dynamic transportation process is inherently complex. Thus, modeling this process can be challenging and computationally demanding. The objective is to build a balanced model that reflects the realism of the dynamic transportation process, and is still computationally tractable and can be implemented in reality by decision-makers. On the other hand, the users of the transportation network require reasonable travel times within the network to reach their destinations. The output of the model should align with the decision-maker and the user requirements.

In this paper, we propose a novel approach to model the evacuation process in order to help decision-makers allocate demands on the available capacity resources to reduce the

congestion effect and find the optimal network clearance time. Specifically, a mixed-integer linear programming (MILP) model is developed as a dynamic traffic assignment (DTA) model that we call a latency-based model (LBM). To the best of our knowledge, there is no mathematical programming modeling approach that computes the estimated time each group of evacuees spends on each route. Most of the mathematical programming DTA models find the network clearance time (NCT), and some models compute the estimated average travel time (ATT) and average evacuation time (AET) of the evacuees [1]. In this proposed model, evacuees use the set of shortest routes to reach their destination. There are many algorithms that can find the set of shortest routes [2]. Moreover, the travel time on any road segment is load-dependent as a function of the flow. The function used is a modified version of the Bureau of Public Roads (1964) function proposed by [3]. Our model is capable of propagating the delay that takes place in downstream road segments to the upstream segments along the predefined routes. Using small network examples, the results of the model are compared with the cell transmission model (CTM) introduced by [4,5], which was later modified to a linear programming (LP) model by [6]. We also show that the CTM model regulates the entry to a road segment rather than slowing the traffic along the road segment, which indicates that the CTM model is insensitive to the length of a congested road segment. The model is also tested on a real-world network, and the results are compared with the CTM. Further, sensitivity analysis is implemented by changing the number of groups to observe the behavior of the ATT and AET.

This paper is organized as follows: The state-of-the-art and relevant studies are listed in Section 2. A new modeling approach is introduced and discussed in Section 3. Then, a reduced complexity version of the model is introduced in Section 4. Next, trivial examples are used to illustrate the model and compare it with the CTM in Section 5.1. In addition, a real-world network is used for experimentation, and the reduced complexity model is compared with the original model in Section 5.2. Then, the computational complexity is discussed in Section 5.3. Finally, conclusions and future work are discussed in Section 6.

2. Literature Review

Most evacuation models in mathematical programming are based on static and dynamic traffic assignments. See [7–12] for static and dynamic traffic assignment examples. There are several objectives in these models, such as system optimal (SO), user equilibrium (UE), nearest allocation (NA), and constrained system optimal (CSO). The objective in SO, as defined by [13], is to minimize the total evacuation time of evacuees to minimize the NCT. In UE, the evacuation time for each group or individual on all routes is minimized so that no individual can improve their travel time by changing routes (Nash equilibrium). UE is equivalent to min-max fairness (MMF), where the maximum evacuation time of all evacuees is minimized until it cannot be improved any further. Then, the next group of evacuees' evacuation time that can be improved is minimized until they cannot be improved, and so on until all evacuation times of all evacuees are minimized [14,15]. Evacuees are assigned to the nearest shelter or safe destination in NA [16]. The models SO and UE/NA are contradicting since the SO does not consider the distribution of the individual evacuation times. However, CSO considers both SO and UE/NA since additional constraints are added to redistribute the evacuees to acceptable routes proposed by [7]. The drawback of SO is that the model does not consider the congestion in different parts of the network as the model objective is to minimize the network clearance time. Hence, parts of the network can be highly congested, leading to longer evacuation times [17].

One of the first attempts to model the DTA as a discrete-time SO mathematical program was by [18,19]. The M-N model captures the traffic propagation due to congestion through a link exit function, and the travel time is represented through the link performance function

of the traffic volume. The model has been extended and investigated with different exit flow functions, link travel time models, and first-in-first-out (FIFO) properties by [20–22]. In general networks, additional constraints of a non-convex structure are imposed to maintain the FIFO requirement, which can lead to greater computational complexity, as discussed by [23]. Another issue that commonly occurs in discrete SO-DTA is the traffic holding-back, where the traffic on one route is delayed for an unreasonable time in favor of other traffic since there is no restriction on how long a group of evacuees can be delayed. Both FIFO and traffic holding-back are discussed by [24]. Another modeling approach of the DTA is the point queue (PQ) model. The assumption in this model is that the time spent in the network is the travel time at free-flow speed plus the waiting time in the queue. The vehicle waits in an exit queue on the link until it is possible to move forward to the next link based on the capacity and the cost of the link. See [25,26] for more illustrations on PQ models.

One of the widely accepted approaches for modeling the dynamic evacuation process is the CTM developed by [4,5] based on [27,28] (LWR) hydrodynamic model of traffic flow. The model is called CTM since the network is divided into homogeneous cells. On the tick of a clock, the evacuees in one cell move to the next cell once the capacity allows them to move forward. Ziliaskopoulos [6] introduced a linear programming (LP) formulation of CTM with a single destination and SO objective. Ukkusuri and Waller [29] proposed a linear dynamic user equilibrium network design problem (UE-NDP) based on the CTM model. However, the M-N model and the CTM are based on a similar concept of traffic movement and delay propagation. Nie [30] shows that incorporating additional constraints to the linearized M-N model results in relaxed CTM and proposes an algorithm to solve the issue of flow holding back. Therefore, both models are generally similar in the basic concept since CTM can be derived from the original M-N model. Essential information lacking in these models is the total time each group of evacuees spends in the network until they reach their destination.

The motivation of this research is to develop a model that captures the desirable properties of both static and dynamic traffic assignment models. The static traffic assignment models use the load-dependent nonlinear travel time functions but do not reflect the reality of the traffic congestion propagation effect. The DTA models consider the propagation by controlling the movement of the traffic but do not provide enough information about the evacuees. The estimated time for each group of evacuees, for example, to reach their destination, is unknown in CTM, which can result in very long evacuation times for some evacuees and lead to selfish behavior. Selfish routing has regained great interest in recent years after Wardrop's first principle UE. Game theory or network games is a common approach that addresses selfish routing (see [31–34]). Also, other objectives are tested to be compared with the NCT. Hence, a new approach is introduced to express the congestion in a more obvious and realistic way.

More recent studies introduce a modified version of the CTM for better accuracy [35–37]. Shrike et al. [35] propose a new model, Arterial Cell Transmission Model (ACTM), that extends the capability of the CTM to better capture the essence of arterial networks. Wu et al. [36] study the case of using adaptive cruise control and cooperative adaptive cruise control using the CTM in the case of congestion of mixed traffic flow of both connected automated vehicles and human-driven vehicles. Alimardani and Baras [37] propose a modified version of the CTM that is based on the piecewise approximation of the flow–density relation. Bayram and Yaman [38] consider risk as the main objective in their CTM model.

Another recent study proposes a multi-objective optimization model aimed at reducing risk during the evacuation process, called the Risk Reduction Model (RRM), where problem-specific indicators for screening for optimal solutions are considered [39]. The study uses the Ogu area in Tokyo as a case study, where the high density of wooden structures increases

the risks of building collapse and fire spread after an earthquake. Another study focuses on evacuating vulnerable residents using both electric and conventional vehicles [40]. It is classified as a vehicle routing problem with energy constraints (VRPEC) since the electric vehicles used in this research do not require recharging during operation, ensuring rapid evacuation, which is crucial. Another study proposed a model that incorporates several features, including vehicle reuse, multi-trip and split delivery scenarios for evacuees and emergency relief items, uncertainty in evacuation demands, and closing time windows at evacuation points to identify an optimal solution to minimize loss and damage [41]. A study presents a crowdsourcing delivery optimization model that considers the bounded rationality of crowdsourcing couriers [42]. It analyzes the couriers' participation rate under three types of uncertainties and assists logistics companies in reducing delivery costs by adjusting the delivery price per parcel and delivery distance while ensuring a certain level of delivery coverage. The reader is referred to a full review of transit-based evacuation planning in emergency logistics management [43].

Recent research has focused on optimizing evacuation strategies for various scenarios using mixed-integer programming (MIP) approaches. A study introduces a mixed-integer programming model to optimize the evacuation of isolated communities using a coordinated fleet of heterogeneous recovery resources [44]. This research evaluates the structure-based heuristics to solve the deterministic and stochastic versions of the isolated Community Evacuation Problem (ICEP). Another study proposes a goal programming model for the early evacuation of vulnerable people and the distribution of relief supplies during a wildfire, which is a dynamic, multi-modal, and multi-criteria problem that considers the classification of evacuees and supplies as well as the dynamic arrival of both evacuees and supplies over time [45].

From the previous studies listed in this paper, the research gaps identified in this study lie in the fact that dynamic models, such as the Cell Transmission Model (CTM), do not account for the total travel time or evacuation time for each group of evacuees. These crucial metrics are typically incorporated in static evacuation models. Consequently, this study proposes a model that integrates the strengths of both static and dynamic models.

3. Evacuation Model (LBM I)

In this section, a novel evacuation modeling approach is introduced. Before running the model, the network is preprocessed by identifying all the hub nodes in the network and adding artificial hub nodes if necessary. Then, the shortest routes from source nodes to terminal nodes are identified. The hub nodes are identified or added so that the travel time at free-flow speed between each consecutive pair of hub nodes is constant. Once a group of evacuees passes through a hub node on a certain route, this group enters a new road segment with time increments of one-time units. The time unit is decided by the traveling time between two of the consecutive hub nodes at free-flow speed. However, the evacuees may be delayed by more than one-time unit to travel between two hub nodes due to congestion.

Since the travel time is load-dependent, the travel time function (1) is incorporated into the model. The travel time function, also known as the BPR function, describes the relationship between the volume of traffic and the travel time used by the U.S. Department of Commerce Bureau of Public Roads (1964). The travel time $T(f)$ with traffic volume f on a road segment is described as follows:

$$T(f) = T^0 \left(1 + \alpha \left(\frac{f}{c} \right)^\beta \right), \quad (1)$$

where T^0 is the travel time on a road segment at free-flow speed under normal road conditions, given the capacity c of the road segment and α and β are turning parameters describing road characteristics with $\alpha \geq 0$ and $\beta \geq 0$. Those parameters are set to 0.15 and 4, respectively, by the U.S. Department of Commerce Bureau of Public Roads (1964).

Since this function is non-linear, we approximate it through a linear piecewise approximation, given that each linear segment is represented by a slope and intercept, as shown in Figure 1. Note that f is the flow volume, and $T(f)$ is the travel time function (1). The accuracy of the output increases as the number of linear segments increases. These linear segments intercept at f_1 , f_2 , and f_3 , for example.

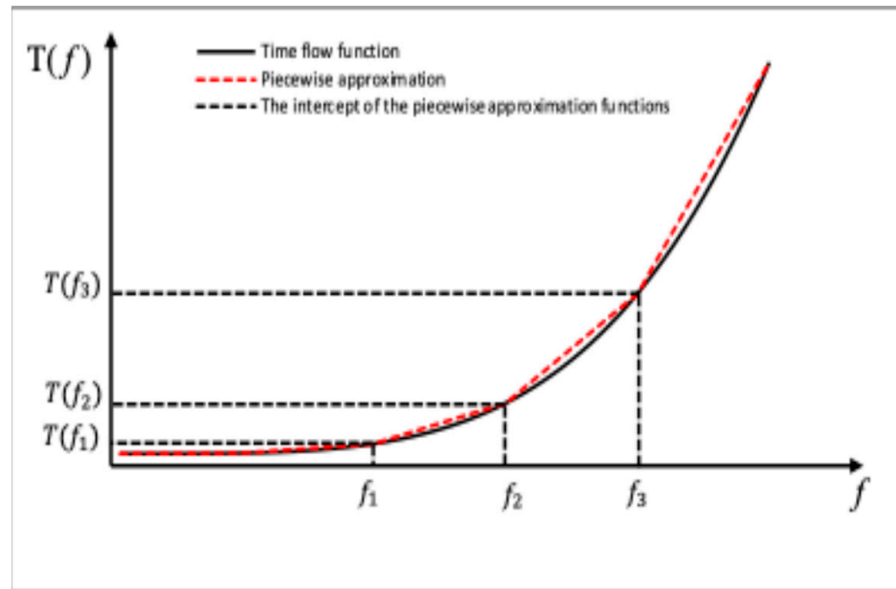


Figure 1. Linearizing the travel time function using piecewise linear approximation.

3.1. LBM I Model Definition

Given a graph $G = (N, A)$ with a set of nodes N and a set of directed arcs A , each arc $a \in A$ connects two nodes $i, j \in N$, where $a = (i, j)$. The nodes of the network are composed of a set of source nodes $N_S \subset N$, a set of terminal nodes $N_T \subset N$, and a set of hub nodes $N_H \subset N$, given that $N_S \subset N_H$ and $N_T \subset N_H$ since the evacuees are allowed to enter or exit through a hub node. Given a set of communities K to be evacuated, R_k is the set of routes that community k can use, where R is the set of shortest routes in the networks from N_S to N_T . $T = \{1, \dots, t_e\}$ is the set of times when evacuees are evacuated, given that t_e is the time when the last group of evacuees is evacuated and $H = \{1, \dots, h_e\}$ is the set of times evacuees are spending in the network, given that h_e is the hub when the last group of evacuees reaches the safe destination. When the time $t \in T$ equals 1, the evacuation process starts. The time path forms a network, and each time segment connects two hubs $h, g \in H$ where $(h, g) \in H_p$. The set V is the traffic volume set, and each element in this set is decided based on the number of vehicles passing per time unit. The link (i, j) on a route is linked to the time of evacuation t from hub h to hub g through the tuple S given that $(i, j, t, h, g) \in S$. More illustration of time path constraints will be given in the example in Section 3.

3.1.1. Parameters and Sets of LBM I Model

- K The set of communities
- R The set of shortest routes from the source nodes to the terminal nodes
- V The set of traffic volumes

- U_B The set of upper bounds based on road capacity where u^v is the upper bound of the traffic volume $v \in V$
- L_B The set of lower bounds based on road capacity where l^v is the lower bound of traffic volume $v \in V$
- D The set of linear segments of the piecewise approximation to the BPR function
- m^d The slope of the linear segment $d \in D$ of the piecewise approximation
- b^d The intercept of the linear segment $d \in D$ of the piecewise approximation
- μ The minimum number of evacuees to be evacuated in any group
- ρ The time in minutes to travel from one hub to the next hub and the system clock
- c_{ij} The time to travel from node i to node j on the link $(i, j) \in A$ at free-flow speed
- C_r The time to travel on route r from source to destination at free-flow speed
- Q_k The population of community k

3.1.2. Set of Variables of LBM I Model

- x_{ijhg}^{ktrv} A non-negative variable represents the number of evacuees from community k evacuated at time t on route r with traffic volume v on arc (i, j) on time path segment (h, g) .
- x_{ijh}^t A non-negative variable represents the number of evacuees on arc (i, j) at hub h
- f_r^{kt} A non-negative variable represents the number of evacuees of community k on route r evacuated at time t
- y_{ijh}^v A binary variable equals 1 if the evacuees on arc (i, j) at hub h is within traffic volume v
- z_{ijhg}^{ktrv} A binary variable equals 1 if the evacuees in community k evacuated at time t are allowed to pass on arc (i, j) on route r at time path segment (h, g) within traffic volume v and 0 otherwise
- τ_{ijh} A non-negative variable represents the latency on arc (i, j) at hub h transferred to the group of evacuees that follows
- $\hat{\tau}_{ijh}$ A non-negative variable represents the slack latency on arc (i, j) at hub h not transferred to the group of evacuees that follows
- τ_{ijh}^{ktr} A non-negative variable represents the latency of the group evacuated from community k on route r at time t on arc (i, j) at hub h
- s_{ijh}^{ktr} A non-negative variable represents the slack variable to complement the latency of the group evacuated from community k on route r at time t on arc (i, j) at hub h
- l_r^{kt} A non-negative variable represents the latency on a full route r of a community k evacuated at time t
- e_r^{kt} A non-negative variable represents the travel time of community k on route r evacuated at time t
- e_r^{kt} A non-negative variable represents the evacuation time of community k on route r evacuated at time t
- E A non-negative variable represents the network clearance time

3.2. Constraints of LBM I Model

The objective of this model is subjected to several constraints that work as the limitations that define the feasible space where the optimal solution exists. These constraints also compute the evacuation time for each group of evacuees and add the propagation effect of delay on the following groups of evacuees.

3.2.1. Flow Conservation Constraints

In the flow conservation constraints (2), evacuees' hub \hat{g} is greater than h since the evacuees pass through a hub node. The hub \hat{g} equals h if the evacuees pass through a non-hub node in the flow conservation constraint (3). Hence, exiting evacuees from node i follow one time path. Every community to be evacuated has a population size of Q_k as

seen in constraint (4).

$$\sum_{\hat{g}|(h,\hat{g})\in H_P} x_{ijh\hat{g}}^{ktrv} - \sum_{g|(g,h)\in H_P} x_{jigh}^{ktrv} = \begin{cases} f_r^{kt} & \text{if } i \in N_S \\ -f_r^{kt} & \text{if } i \in N_T \\ 0, & \text{otherwise} \end{cases} \quad \begin{matrix} \forall k \in K, v \in V, r \in R, \\ \forall (j,i), (i,\hat{j}) \in r, \hat{j} \in N_H, \\ \forall t, h, g | (i,j,t,h,g) \in S \end{matrix} \quad (2)$$

$$x_{ijh\hat{g}}^{ktrv} - \sum_{g|(g,h)\in H_P} x_{jigh}^{ktrv} = 0 \quad \begin{matrix} \forall k \in K, v \in V, r \in R, \\ \forall (j,i), (i,\hat{j}) \in r, \hat{j} \notin N_H, \\ \forall t, h, g | (i,j,t,h,g) \in S \end{matrix} \quad (3)$$

$$\sum_{t \in T} \sum_{r \in R} f_r^{kt} = Q_k \quad \forall k \in K \quad (4)$$

3.2.2. Networks Link Constraints

Since all the evacuees share the same road network, constraint (5) sums all evacuees from all communities k evacuated at different times t with all traffic volumes v using all the routes r passing through the arc (i, j) at hub h to the variable x'_{ijh} .

$$x'_{ijh} = \sum_{r \in R} \sum_{k \in K} \sum_{v \in V} \sum_{t|(i,j,t,h,g) \in S} x_{jihg}^{ktrv} \quad \begin{matrix} \forall (i,j) \in A, \\ \forall h, g | (i,j,t,h,g) \in S \end{matrix} \quad (5)$$

3.2.3. Flow Volume Constraints

The amount of the flow passing through the arc (i, j) is decided by the traffic volume variable y_{ijh}^v . If the flow x'_{ijh} falls between the upper bound u^r and the lower bound l^v of traffic volume v , then y_{ijh}^v equals 1 as shown in constraints (6) and (7) given that M is a significantly large number. The evacuees passing on arc (i, j) at hub h are allowed to pass through one traffic volume as seen in constraint (8).

$$x'_{ijh} \geq \sum_{v \in V} l^v y_{ijh}^v \quad \forall (i,j) \in A, h \in H \quad (6)$$

$$x'_{ijh} \leq \sum_{v \in V} u^v y_{ijh}^v + M(1 - y_{ijh}^v) \quad \forall (i,j) \in A, h \in H \quad (7)$$

$$\sum_{v \in V} y_{ijh}^v \leq 1 \quad \forall (i,j) \in A, h \in H \quad (8)$$

3.2.4. Path Latency Constraints

To find the latency τ_{ijh} on arc (i, j) at hub h , the inventory constraint (9) is used. The latency of an arc (i, j) at hub h equals the required time for evacuees to travel on the arc based on their volume, adding the latency of the evacuees on the same arc at hub $h - 1$ and subtracting the time they would spend at a free-flow speed. It can be noticed that $\hat{\tau}_{ijh}$ in (10) is bounded by the time evacuees spend on the arc at free-flow speed, but it can be less in case no evacuees are passing on the arc to maintain the constraint feasibility. The initial latency of the arc (i, j) equals 0 in constraint (11).

Note that constraint (9) transfers the effect of congestion to the group of evacuees that follows. As the link becomes more congested, the latency increases; then, it is added to the total latency of the following group of evacuees. Although the evacuees are not delayed by the earlier groups on the upstream links of the congested link, the delay is added once they pass the congested road segment.

$$\tau_{ijh} = c_{ij} t_{ijh} + \tau_{ijh-1} - \hat{\tau}_{ijh} \quad \forall (i,j) \in A, \forall h \in H \quad (9)$$

$$\hat{\tau}_{ijh} \leq c_{ij} \quad \forall (i,j) \in A, \forall h \in H \quad (10)$$

$$\tau_{ijh} = 0 \quad \forall (i,j) \in A, h = 0 \quad (11)$$

To find the travel time on a road segment based on the traffic volume, the piecewise approximation to the BPR convex function is used. Since the function is convex, the travel

time t_{ijh} on arc (i, j) at hub h can be found as seen in constraint (12).

$$t_{ijh} \geq m^d x'_{ijh} + b^d \quad \forall (i, j) \in A, \forall h \in H, \forall d \in D \tag{12}$$

3.2.5. Time Path Constraints

All evacuees of community k on arc (i, j) at time h evacuated at time t on route r can pass through one time path as shown in constraints (13) and (15) given that M is a sufficiently large number. Hence, no part of the group is delayed or outrun the rest of the group. In constraint (14), each group of evacuees is bounded by a minimum number μ decided by the decision-maker. In constraint (16), the evacuees follow one time path based on the traffic volume decided by the set of constraints (6) and (7).

$$x_{ijhg}^{ktrv} \leq M z_{ijhg}^{ktrv} \quad \forall (i, j) \in A, \forall r \in R, \forall t \in T, \forall h \in H, \forall k \in K, \forall d \in D_T \tag{13}$$

$$x_{ijrhg}^{ktrv} \geq \mu z_{ijhg}^{ktrv} \quad \forall (i, j) \in A, \forall r \in R, \forall t \in T, \forall h \in H, k \in K \tag{14}$$

$$\sum_{v \in V} z_{ijhg}^{ktrv} \leq 1 \quad \forall (i, j) \in A, \forall r \in R, \forall t \in T, \forall k \in K \tag{15}$$

$$x_{jihg}^{ktrv} \leq M y_{ijh}^v \quad \forall (i, j) \in A, \forall r \in R, \forall t \in T, \forall (h, g) \in H_p, \forall k \in K, \forall v \in V \tag{16}$$

3.2.6. Evacuees Latency Constraints

The latency on a route r of a community k evacuated at time t in constraint (17) is the sum of the latencies (transferred and non-transferred) of the evacuees on that route in the network. Since all communities evacuated at various times using different routes share the same network, the latency of a community k on route r is a subset of the latencies of the network. To extract the latencies of a specific group of evacuees, the variable z_{ijhg}^{ktrv} is used to identify the time path that the evacuees followed, as shown in constraints (18)–(20).

$$l_r^{kt} = \sum_{(i,j) \in r} \sum_{h \in H} \tau_{ijh}^{ktr} \quad \forall t \in T, \forall r \in R_k, \forall k \in K \tag{17}$$

$$\tau_{ijh} + \hat{\tau}_{ijh} = \tau_{ijh}^{ktr} + s_{ijh}^{ktr} \quad \forall (i, j), \forall r \in R, \forall (i, j) \in A, \forall t \in T, \forall h \in T_H, \forall k \in K \tag{18}$$

$$\tau_{ijh}^{ktr} \leq M z_{ijhg}^{ktrv} \quad \forall (i, j) \in A, \forall p \in P, \forall t \in T, \forall h \in H, k \in K \tag{19}$$

$$s_{ijh}^{ktr} \leq M \left(1 - z_{ijhg}^{ktrv}\right) \quad \forall (i, j) \in A, \forall r \in R, \forall t \in T, \forall h \in H, \forall k \in K \tag{20}$$

3.2.7. Evacuation Constraints

The time required to travel for each group of evacuees evacuated from community k on route r at time t to reach their destination is the travel time on route r at free-flow speed in addition to the latency as shown in constraint (21). The evacuation time for each group of evacuees evacuated from community k on route r at time t to reach their destination is the waiting time since the start of the evacuation process, the travel time on route r at free-flow speed, and the latencies on the route as seen in constraint (22). To minimize the network clearance time, the maximum evacuation time is minimized as shown in constraint (23).

$$e_r^{kt} = C_r z_{ijhg}^{ktrv} + l_r^{kt} \quad \forall k \in K, \forall r \in R, \forall (i, j) \in A, \forall r, i \in N_S, \forall t, h, g | (i, j, t, h, g) \in S \tag{21}$$

$$e_r^{kt} = \rho(t-1) z_{ijhg}^{ktrv} + C_r z_{ijhg}^{ktrv} + l_r^{kt} \quad \forall k \in K, \forall r \in R, \forall (i, j) \in A, \forall r, i \in N_S, \forall t, h, g | (i, j, t, h, g) \in S \tag{22}$$

$$e_r^{kt} \leq E \quad \forall k \in K, \forall r \in R, \forall t \in T \tag{23}$$

The set of constraints (24) prevents later evacuees from preceding earlier evacuees on the same route, stating that the volume of the later evacuees is greater than or equal to the earlier evacuees or no evacuees follow them.

$$y_{ijh}^v \leq \sum_{q \in V | q \geq v} y_{ij(h+1)}^q + y_{ij(h+1)}^0 \quad \forall (i, j) \in A, \forall h = 1, \dots, t_e - 1, \quad \forall v \in V \tag{24}$$

Lastly, the following are non-negativity constraints (25) and binary variables constraints (26).

$$x_{ijhg}^{ktrv}, x'_{ijh}, f_r^{kt}, \tau_{ijh}, \hat{\tau}_{ijh}, \tau'^{ktr}_{ijh}, \quad \forall k \in K, \forall r \in R, \forall (i, j) \in A, \tag{25}$$

$$s_{ijh}^{ktr}, l_r^{kt}, e_r^{kt}, e_r'^{kt}, E \geq 0 \quad \forall v \in V, \forall t, h, g | (i, j, t, h, g) \in S$$

$$y_{ijh}^v, z_{ijhg}^{ktrv} \in \{0, 1\} \quad \forall k \in K, \forall r \in R, \forall (i, j) \in A, \tag{26}$$

$$\forall v \in V, \forall t, h, g | (i, j, t, h, g) \in S$$

Before building the MILP model, all the possibilities of all groups of evacuees passing through road and time networks are built and stored into sets. When building the model, the constraints refer to these sets.

3.3. Objective Functions

The objective of the model is to minimize the network clearance time (NCT) given that E is the total travel time of the last group arriving at the safe destination since the beginning of the evacuation process, as seen in the objective function (27).

$$Min \ NCT = E \tag{27}$$

However, different objectives are experimented. The average travel time (ATT) and the average evacuation time (AET) for each group of evacuees are incorporated in the model as seen in objectives (28) and (29), respectively. The sum of z_{ijhg}^{ktrv} for all $i \in N_S$ is the number of groups to be evacuated, given that the minimum number of groups to be evacuated is one group. The total number of groups z_{ijhg}^{ktrv} is decided by the decision-maker, which makes the constraints (28) and (29) linear.

$$Min \ ATT = \frac{\sum_{k \in K} \sum_{r \in R} \sum_{t \in T} e_r^{kt}}{\sum_{k \in K} \sum_{r \in R} \sum_{(i,j) \in r | i \in N_S} \sum_{t,h,g | (i,j,t,h,g) \in S} z_{ijhg}^{ktrv}} \tag{28}$$

$$Min \ AET = \frac{\sum_{k \in K} \sum_{r \in R} \sum_{t \in T} e_r'^{kt}}{\sum_{k \in K} \sum_{r \in R} \sum_{(i,j) \in r | i \in N_S} \sum_{t,h,g | (i,j,t,h,g) \in S} z_{ijhg}^{ktrv}} \tag{29}$$

3.4. Illustrative Example

Consider a network with five nodes and four arcs, as shown in Figure 2. Suppose that the population in the source node n1 is evacuated to the shelter in the terminal node n5. Node n1 is a source node, node n5 is a terminal node, and n1, n2, n4, n5 are hub nodes. The time to travel from n1 to n2 at free-flow speed is 60 min, and the time to travel from n2 to n4 is 60 min. The total travel time, at free-flow speed, from n1 to n5 is 180 min. The travel time based on the number of evacuees is shown in Table 1. The traffic can fall into three volumes. The lower bounds set of the traffic volumes is $L_B = \{0, 1, 4351, 4901\}$, and the upper bounds set is $U_B = \{0, 4350, 4900, 5200\}$.

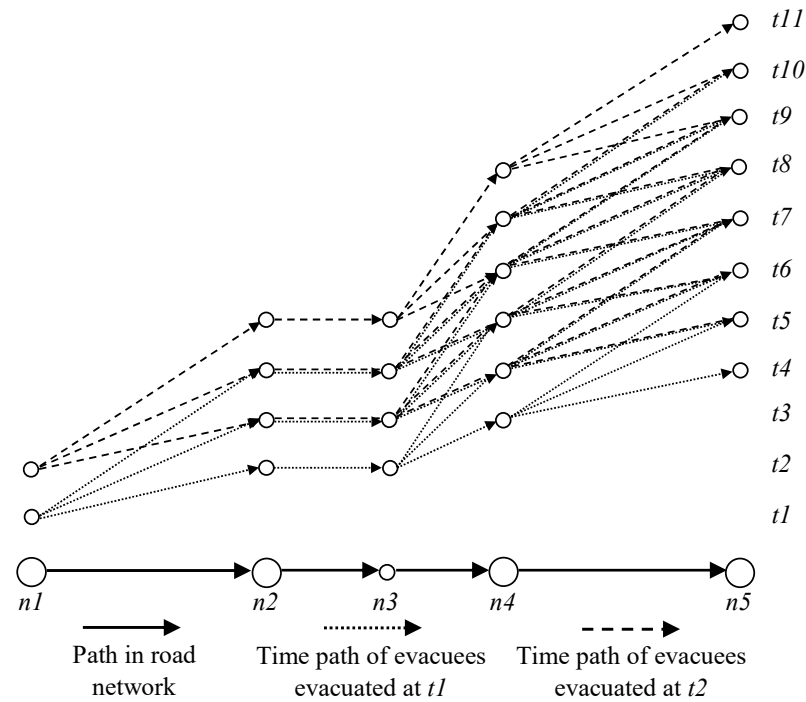


Figure 2. A small network example with 5 nodes and 4 arcs.

Table 1. Travel time between each pair of hub nodes based on the number of evacuees.

d	Number of Vehicles	Travel Time
1	2200	0.0167
2	4350	1
3	4650	1.5
4	4900	2
5	5200	3

The model is tested on three different population sizes in three scenarios, A, B, and C, assuming that in each scenario, the population is divided into two groups, as shown in Table 2. The first group is evacuated at $t1$ and the second group is evacuated at $t2$. As shown in scenario A in Figure 2, the population of 8500 is divided into two groups of 4350 and 4150 evacuees with the same traffic volume. The latency of the first group is 180 min, resulting from a delay of 60 min between every two consecutive hub nodes. The second group’s latency is 163.54 min, resulting from the delay by their own congestion. The delay of the first group is not transferred to the second group since the latency of the first group is less than or equal to the travel time at free-flow speed, as seen in constraint (10). In scenario B, the population is 9500, and the first group of evacuees’ traffic volume is 2 resulting in a delay of 254.7 min. The second group of evacuees falls in traffic volume 3 with a latency of 385.5 min delayed partially by the first group of evacuees since there is a gap of time between them. The first group in scenario C is delayed by 180 min between every pair of consecutive hub nodes, for a total of 540 min. The second group is delayed by 540 min in addition to the transferred delay from the first group of 360 min. The travel time is the latency in addition to the travel time at free-flow speed, the evacuation time is the travel time in addition to the waiting time of 60 min, and the NCT is the maximum evacuation time. We conclude that the travel time grows exponentially as the number of evacuees in a group becomes larger.

Table 2. Results of the example network of the three scenarios.

Scenario	Population Size	Time	Number of Evacuees	Latency	Travel Time	Evacuation Time	NCT
A	8500	1	4350	180.00	360	360	403.54
		2	4150	163.54	343.54	403.54	
B	9500	1	4599	254.7	434.7	434.7	625.5
		2	4901	385.5	565.5	625.5	
C	10400	1	5200	540	720	720	1140
		2	5200	900	1080	1140	

Figure 3 illustrates the time path of the groups of evacuees in all three scenarios. In the experimentation section, other objectives are tested, resulting in different distributions of evacuees with the same network clearance time.

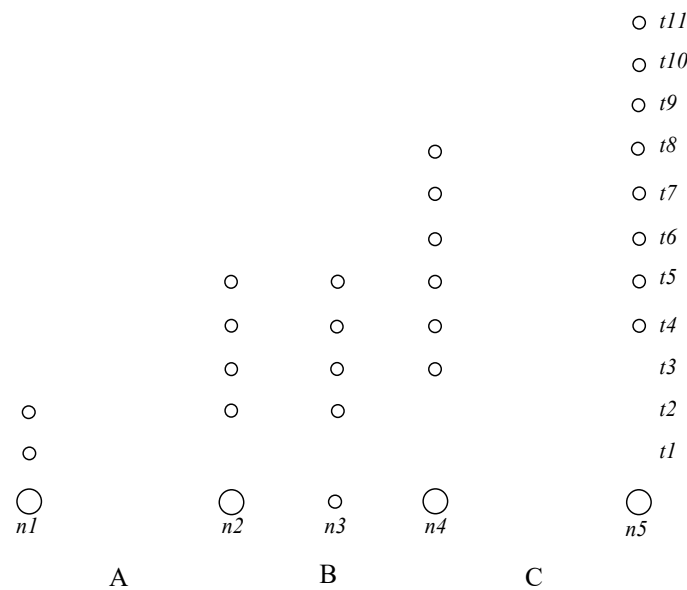


Figure 3. Results of the network example of the 3 scenarios.

As seen in Figure 3, the evacuees evacuated from node 1 at time 1 either reach node 2 at time 2 at free-flow speed, reach at time 3 under moderate congestion, or reach at time 4 under high congestion. The evacuees must stay in one group to find their travel time and keep track of them. The binary variable z_{ijhg}^{ktrv} indicates the time path the evacuees follow based on their volume v . Hence, the number of binary variables used increases with the number of routes r , times of evacuation t , number of communities k , and the length of route for all $(i, j) \in r$. This motivates us to develop the model to reduce its complexity. Computational complexity is discussed in a later section.

4. Evacuation Model (LBM II)

In this section, we propose a reduced complexity version of the LBM in order to help decision-makers allocate demands on the available capacity resources for large-scale problems. Specifically, a linear programming (LP) model is developed as a dynamic traffic assignment (DTA) model, as illustrated in Figure 4. The results of the original model and the less complex version of the model are compared. The computational time for both models is included in the comparison. In addition, the results of the model are compared with the known cell transmission model.

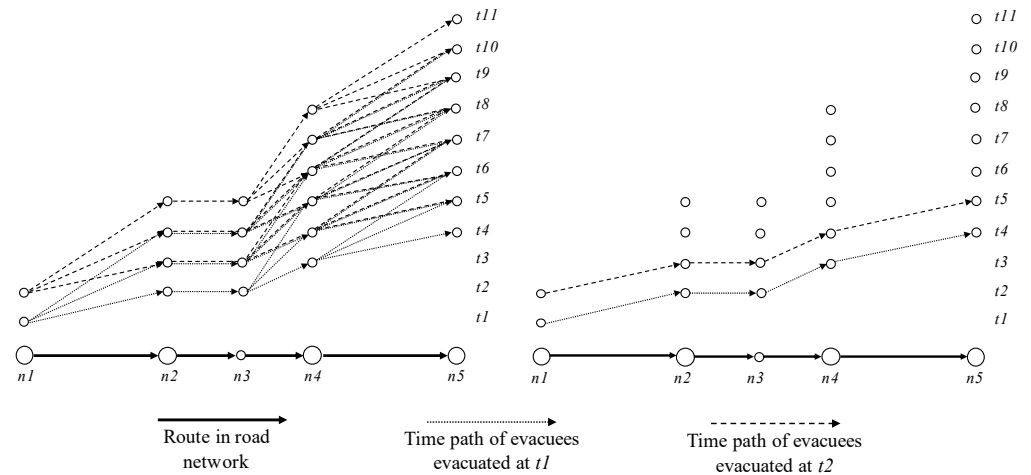


Figure 4. The time paths of the full model and the reduced model.

4.1. LBM II Model Definition

The model definition of LBM II is similar to that of LBM I. Only the tuple S is reduced to $(i, j, t, h) \in S$.

4.1.1. Parameters and Sets of LBM II Model

- K The set of communities
- R The set of shortest routes from the source nodes to the terminal nodes
- D The set of linear segments of the piecewise approximation to the BPR function
- m^d The slope of the linear segment $d \in D$ of the piecewise approximation
- b^d The intercept of the linear segment $d \in D$ of the piecewise approximation
- u The maximum number of evacuees on any arc
- μ The minimum number of evacuees to be evacuated in any group
- ρ The time in minutes to travel from one hub to the next hub node at free-flow speed and the system clock
- c_{ij} The time to travel from node i to node j on the link $(i, j) \in A$
- C_r The time to travel on route r from source to destination at free-flow speed
- Q_k The population of community k .

4.1.2. Set of Variables of LBM I Model

- x_{ijrh}^{kt} A non-negative variable represents the number of evacuees on arc (i, j) on route r at hub h of community k evacuated at time t
- x_{ijh} A non-negative variable represents the number of evacuees on arc (i, j) at hub h
- f_r^{kt} The number of evacuees of community k on route r evacuated at time t
- z_{ijrh}^{kt} A binary variable equals 1 if community k evacuated at time t is allowed to pass on arc (i, j) on route r at hub h , and it equals 0 otherwise
- t_{ijh} A non-negative variable represents the travel time on arc (i, j) at time h based on the piecewise approximated travel time function
- τ_{ijh} A non-negative variable represents the latency on arc (i, j) at hub h transferred to the group of evacuees that follows
- $\hat{\tau}_{ijh}$ A non-negative variable represents the slack latency on arc (i, j) at hub h not transferred to the group of evacuees that follows
- τ_{ijh}^{ktr} A non-negative variable represents the latency of the group evacuated from community k at time t on route r on arc (i, j) at hub h

s_{ijh}^{ktr} A non-negative variable represents the slack variable to remove the effect of latency of the group of evacuees from community k if they do not pass through the arc (i, j) on route r at hub h

l_r^{kt} A non-negative variable represents the latency of the group of evacuees on route r of a community k evacuated at time t

e_r^{kt} A non-negative variable represents the travel time of community k on route r evacuated at time t

e_r^{rkt} A non-negative variable represents the evacuation time of community k on route r evacuated at time t

E A non-negative variable represents the network clearance time.

4.2. Latency-Based Model

$$\text{Min NCT} = E \tag{30}$$

Subject to

$$x_{ijr(h+1)}^{kt} - x_{jirh}^{kt} = \begin{cases} f_r^{kt} & \text{if } i \in N_S \\ -f_r^{kt} & \text{if } i \in N_T, \text{ if } i \in N_H \\ 0, & \text{otherwise} \end{cases} \quad \begin{matrix} \forall r \in R, (i, j) \in A, \forall r, \\ \forall k \in K, \forall t, h | (i, j, t, h) \in S \end{matrix} \tag{31}$$

$$x_{ijrh}^{kt} - x_{jirh}^{kt} = 0, \text{ if } i \notin N_H \quad \forall r \in R, \forall (i, j) \in A, \forall r, k \in K, \forall t, h | (i, j, t, h) \in S \tag{32}$$

$$\sum_{t \in T} \sum_{r \in R} f_r^{kt} = Q_k \quad \forall k \in K \tag{33}$$

$$x'_{ijh} = \sum_{r \in R} \sum_{k \in K} \sum_{t | (i, j, t, h) \in S} x_{ijrh}^{kt} \quad \forall (i, j) \in A, \forall h \in H \tag{34}$$

$$\tau_{ijh} = c_{ij} t_{ijh} - \hat{\tau}_{ijh} \quad \forall (i, j) \in A, \forall h \in H \tag{35}$$

$$\hat{\tau}_{ijh} \leq c_{ij} \quad \forall (i, j) \in A, \forall h \in H \tag{36}$$

$$\tau_{ijh} = 0 \quad \forall (i, j) \in A, \forall h = 0 \tag{37}$$

$$t_{ijh} \geq m^d x'_{ijh} + b^d \quad \forall (i, j) \in A, \forall h \in H, \forall d \in D \tag{38}$$

$$\tau_{ijh} \geq \tau_{jlv} - \rho(1 + h - v) \left(1 - z_{ijrh}^{kt} \right) \quad \begin{matrix} \forall h, v \in H | h \geq v, \forall r \in R, \\ \forall t \in T, \forall (i, j, t, h) \in S \end{matrix} \tag{39}$$

$$x_{ijph}^{kt} \leq u z_{ijrh}^{kt} \quad \begin{matrix} \forall i \in N_S, (i, j) \in A, \forall r \in R, \\ \forall t, h | (i, j, t, h) \in S, \forall k \in K \end{matrix} \tag{40}$$

$$x_{ijph}^{kt} \geq \mu z_{ijrh}^{kt} \quad \begin{matrix} \forall i \in N_S, \forall (i, j) \in A, \forall r \in R, \\ \forall t, h | (i, j, t, h) \in S, \forall k \in K \end{matrix} \tag{41}$$

$$l_r^{kt} = \sum_{(i, j) \in r} \sum_{h \in H} \tau_{ijh} \quad \forall t \in T, \forall k \in K, \forall r \in R_k \tag{42}$$

$$\tau_{ijh}^{ktr} + s_{ijh}^{ktr} = \tau_{ijh} + \hat{\tau}_{ijh} \quad \forall (i, j) \in A, \forall h \in H, \forall k \in K \tag{43}$$

$$\tau_{ijh} \leq M z_{ijrh}^{kt} \quad \begin{matrix} \forall (i, j) \in A, \forall k \in K, \\ \forall t, h | (i, j, t, h) \in S \end{matrix} \tag{44}$$

$$s_{ijh} \leq M \left(1 - z_{ijrh}^{kt} \right) \quad \begin{matrix} \forall (i, j) \in A, \forall k \in K, \\ \forall t, h | (i, j, t, h) \in S \end{matrix} \tag{45}$$

$$e_p^{kt} = C_p z_{ijph}^{kt} + l_p^{kt} \quad \begin{matrix} \forall i \in N_S, \forall r \in R, \forall (i, j) \in A, \\ \forall r, t, h | (i, j, t, h) \in S \end{matrix} \tag{46}$$

$$e_r^{kt} = \rho(t - 1) z_{ijrh}^{kt} + C_r z_{ijrh}^{kt} + l_r^{kt} \quad \begin{matrix} \forall i \in N_S, \forall r \in R, \forall (i, j) \in A, \\ \forall r, t, h | (i, j, t, h) \in S \end{matrix} \tag{47}$$

$$\begin{aligned}
 e_r^{kt} &\leq E && \forall k \in K, \forall r \in R, \forall t \in T && (48) \\
 x_{ijrh}^{kt}, x'_{ijh}, f_r^{kt}, \tau_{ijh}, \hat{\tau}_{ijh}, \tau'_{ijh}, &&& \forall (i, j) \in A, \forall k \in K, \forall r \in R, && (49) \\
 s_{ijh}, l_r^{kt}, e_r^{kt}, e_r^{kt}, E \geq 0 &&& \forall t \in T, \forall h \in H, && \\
 &&& \forall (i, j, t, h) \in S && \\
 z_{ijh}^{kt} \in \{0, 1\} &&& \forall (i, j) \in A, \forall k \in K, && (50) \\
 &&& \forall t, h | (i, j, t, h) \in S &&
 \end{aligned}$$

Note that the flow conservation constraints (31) and (32) are slightly modified compared to the original flow conservation constraints. These constraints allow evacuees to follow one time path along the predefined route. Constraint (33) sums all evacuees evacuated at all times on all routes to equal the community population. Evacuees from different communities evacuated at different times from different routes meet on a road segment (i, j) at hub h . The latency τ_{ijh} is the travel time based on the volume of the evacuees subtracting their travel time at free-flow speed as seen in constraint (35). Note that $\hat{\tau}_{ijh}$ can be less than the free-flow speed in case no evacuees pass to maintain the constraint feasibility as shown in constraint (36), given that the initial latency is 0, as seen in constraint (37). The travel time based on the volume is illustrated in constraint (38) since the travel time is a convex function. Constraint (39) transfers the delay to the group of evacuees that follow to propagate the congestion to the upstream road segments. Constraints (40) and (41) use the binary variable z_{ijrh}^{kt} to determine whether it allows the evacuees from community k evacuated at time t to pass through the arc (i, j) on route r at hub h , given that u is the capacity of the road segment and μ is the minimum number of evacuees in a group. The latency of the group from community k evacuated at time t on route r is the sum of latencies along that route, as seen in constraint (42). Since the routes overlap, constraints (43)–(45) are extracted from the network with the help of the indicator variable z_{ijrh}^{kt} . The travel time of a group is the travel time at free-flow speed in addition to the latency, as seen in constraint (46), and the evacuation time is the waiting time since the beginning of the evacuation process in addition to the travel time as seen in constraint (47). The network clearance time E is the maximum evacuation time among all evacuated groups, as shown in constraint (48). Finally, constraints (49) and (50) are the non-negativity constraints.

5. Illustration and Experimentation

In this section, a trivial network is used to illustrate the model. A real-world small network is also used for illustration and experimentation.

5.1. Illustrative Examples

5.1.1. Example 1

Consider the two simple networks as road segments illustrated in Figure 5. Assume that each road segment is composed of two lanes with a capacity of 1750 vehicles/lane/hour. The travel time at free-flow speed from one node to the next node is 60 min, and the travel time increases due to congestion, as illustrated in Table 3. The latency based on the number of vehicles is shown in Table 3. This information is used to approximate the nonlinear BPR flow–travel time function using a piecewise linear approximation. The lane capacity is set to 1750 vehicles/lane/hr, and each link in the network is assumed to consist of two lanes. To find the latency on a road segment, the latency column in Table 3 is multiplied by the travel time on the road segment at free-flow speed. It can be seen as a scalar that adjusts the travel time based on the number of vehicles.

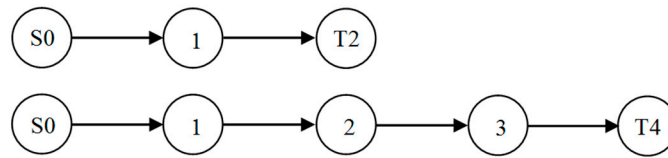


Figure 5. Road segment with 60 min travel time between each pair of consecutive nodes at free-flow speed.

Table 3. Travel time based on the number of vehicles using modified BPR and the shockwave speed to the free-flow speed ratio.

Number of Vehicles	Latency	Speed Ratio δ
0	0	1
2200	0.0167	0.99
4350	1	0.5
4650	1.5	0.4
4900	2	0.33
5200	3	0.25

The number of evacuees is 4900, traveling through the three-node network in Figure 5 from the source node S0 to the terminal node T2, with a total travel time of 120 min under normal conditions. When using the CTM model, we set the link capacity to 5200 vehicles, and the shockwave speed ratio is set to 0.33, as seen in Table 3. The NCT is 300 min, while the NCT of the LBM is 360 min. Now, we assume that the distance is doubled in the network with five nodes to become 240 min under normal conditions, as illustrated in Figure 5. Evacuating 4900 evacuees requires 420 min when using the CTM, and it requires 720 min when using the LBM. Notice that the NCT of the LBM is doubled as the distance is doubled, while the NCT in the CTM is increased by 120 min, which is the distance of the added road segment. We conclude that the CTM does not capture the congestion on the added road segment; it regulates the entry of vehicles at the beginning of the road segment. Then, the vehicles travel the rest of the road segment at free-flow speed, which does not reflect the reality of real-world congestion.

5.1.2. Example 2

Consider the network with seven nodes and seven arcs shown in Figure 6. The population in node S0 is evacuated to the shelter in node T6. Node S0 is a source node, node T6 is a terminal node, and all nodes are set as hub nodes. The time to travel from one node to the next node is 60 min at free-flow speed. The predefined routes are S0-1-3-5-T6 and S0-2-4-5-T6. The total travel time from the source to the terminal on either route in normal conditions is 240 min, and the number of vehicles to be evacuated is assumed to be 15,000.

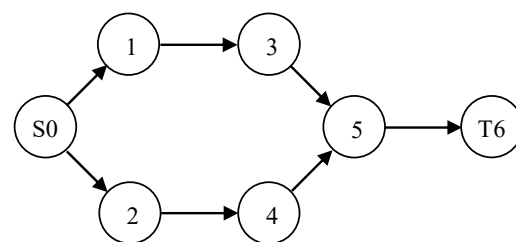


Figure 6. A small network for illustration.

The network consists of seven nodes and seven directed arcs. The optimal NCT is 667.9 min, assuming that there is no congestion at the beginning of the evacuation process,

as seen in Table 4. Note that the first group of evacuees evacuated on both routes does not cause any congestion, which is referred to as latency τ , until they reach the bottleneck arc (5,6), but they cause a delay to themselves of 1 min on the non-bottleneck links on route 1 and 14.72 min on the non-bottleneck links on route 2, which is the slack latency $\hat{\tau}$. Although the delay is 120 min, as the total number of evacuees is 4900, the delay they transfer to the succeeding group is 60 min since the latter are evacuated 60 min later. The second group of evacuees is delayed by 60 min on arcs (3,5) and (4,5) by the first group. Then, they cause a delay of 120 min on the bottleneck arc (5,6). The third group of evacuees is delayed by the first and second groups. There is a 60 min delay on arcs (1,3) and (2,4) due to the propagated delay from the first group, and a delay of 120 min on arcs (3, 5) and (4,5) by the second group that causes a delay of 60 min on the bottleneck arc.

Table 4. The number of evacuees evacuated on each route in each period is illustrated for example 2. The latency in each link is shown in addition to the NCT.

Time	Number of Evacuees (f)		Latency (τ)							Obj. NCT (m)	
			Slack Latency ($\hat{\tau}$)								
			Route 1	Route 2	(0,1)	(0,2)	(1,3)	(2,4)	(3,5)		(4,5)
1	2200	2700	0 1	0 14.72							
2	3000	2200	0 22.9	0 1	0 1	0 14.72					
3	2450	2450	0 7.86	0 7.86	0 22.95	0 1	0 1	0 14.72			667.86
4					60 0	60 0	60 0	60 0	60 0	60 60	
5							120 0	120 0	120 60		
6										60 60	

The summary of the travel time and evacuation time on each route and different evacuation times are presented in Table 5. Note that the travel time is the latency added to the travel time at free-flow speed. The evacuation time is the travel time added to the waiting time since the beginning of the evacuation process. The evacuation time for the groups evacuated in the first period equals the travel time since they are evacuated at the beginning of the evacuation process, while 60 min are added for every period the group of evacuees is waiting to be evacuated.

Table 5. Summary of the results of the second example for each group of evacuees on different routes and evacuation.

Time	Route	Latency	Travel Time	Evacuation Time
1	1	123.00	363.00	363.00
	2	164.16	404.16	404.163
2	1	345.91	585.91	645.91
	2	302.00	542	602.00
3	1	307.86	547.86	667.86
	2	307.86	547.86	667.86

5.1.3. Comparing the LBM with the CTM Model

The LBM is compared with the CTM. The network used for comparison is the network illustrated in Figure 6. Although the number of groups to be evacuated cannot be decided in the CTM, we assume that the total evacuees are divided into six groups evacuated in three periods on two routes. From this assumption, the shockwave speed ratio can be decided based on the travel time, as seen in Table 3. Note that the demand ranges from 500 up to 15,500. When the demand is 500, the NCT is 240 for both models since there is no congestion, and all evacuees can be evacuated in the first period with no delays, as seen in Figure 7. As the demand increases, the NCT increases nonlinearly following the behavior of the BPR function, given that the shockwave speed parameter δ_i is updated for every node $i \in N_R$ for each demand scenario.

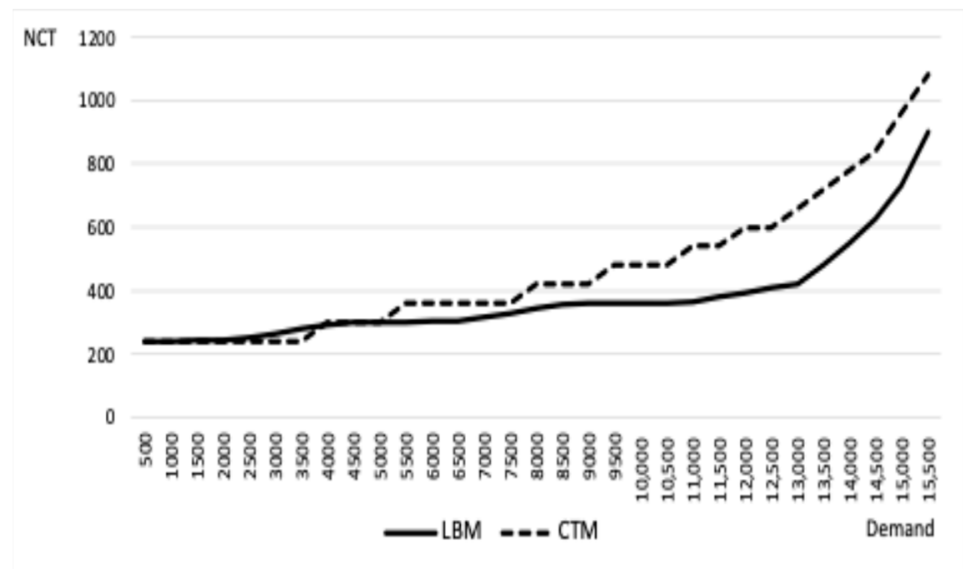


Figure 7. The NCT in minutes for the LBM is compared with the CTM output.

5.2. Experimentation

The network experimented in this section is Tampa City, Florida, and is obtained from Google Maps (2014). Suppose node 1 and 2 populations are evacuated to the incapacitated safe zone in nodes 21–25, as shown in Figure 8; first, the nodes are identified as hub or non-hub nodes. The non-hub nodes set is $N \setminus N_H = \{4, 6, 7, 8, 14, 17\}$, and the remainder of the nodes are hub nodes N_H . Note that nodes 11 and 15 are examples of artificial nodes that have been added to the network as hubs to give a hub increment to the evacuees passing through them and the unit of time ρ is set to 30 min based on the size of the network. The number of all possible simple routes, eliminating loops, from the source node 0 to the sink node 26 is 17. All routes can be used, but in an evacuation process, the set of routes used is the set of shortest routes to minimize the travel time to reach a safe destination. The selected set of shortest routes is shown in Table 6.

The number of evacuees in the community in node 2 is assumed to be 25,000 evacuees. When minimizing the network clearance time E , the model requires three time units, which is equivalent to 1.5 h, to evacuate all the evacuees from the endangered area. Also, the minimum network clearance time is 150 min or 2.5 h until the last group of evacuees reaches the destination, as shown in Table 7.

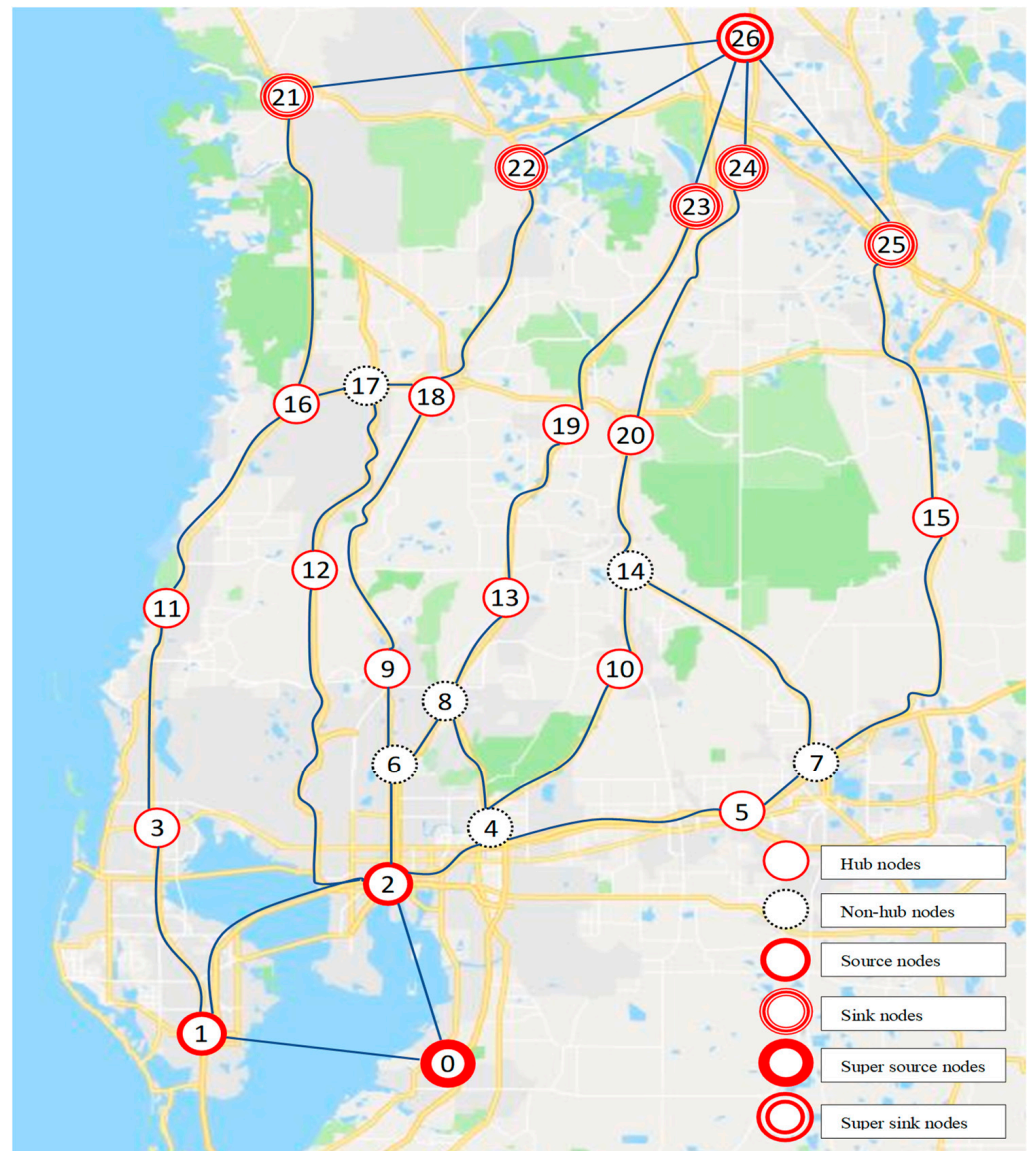


Figure 8. Random network with 27 nodes and 43 bidirected arcs.

Table 6. The set of shortest routes in the Tampa City network from source node 0 to destination node 26.

p	Route	Length (min)
0	0-2-12-17-16-21-26	90
1	0-2-12-17-18-22-26	90
2	0-2-6-9-18-22-26	90
3	0-2-6-8-13-19-23-26	90
4	0-2-4-8-13-19-23-26	90
5	0-2-4-10-14-20-24-26	90
6	0-2-4-5-7-14-20-24-26	90
7	0-2-4-5-7-15-25-26	90

Table 7. Summary of results in minutes with different objectives when minimizing each objective in a different run.

Objective (Minimize)	NCT	ATT	AET	Groups	Computational Time (s)
NCT	150.02	123.32	147.32	15	5.65
ATT	182.00	97.25	127.25	24	16.4
AET	153.00	99.95	121.13	17	6.30

To find the optimal ATT and AET, the ϵ – constraint method is used since the range of the number of groups is known. In the Tampa City network, the evacuation time is three time units when the NCT is minimized. The maximum number of groups to be evacuated is 24 when the evacuation time is fixed to three units, given that the number of routes is eight. The following model is solved to find the optimal solution of ATT in addition to Constraints (31)–(50):

$$Min\ TTT = \sum_{k \in K} \sum_{r \in R} \sum_{t \in T} e_r^{kt} \tag{51}$$

subject to

$$\sum_{k \in K} \sum_{r \in R} \sum_{h \in H} \sum_{t \in T} \sum_{(i,j) \in r} z_{ijrh}^{kt} = \epsilon \tag{52}$$

Since the range of ϵ is known, the total travel time (TTT) in the objective function (51) is minimized while changing the total number of groups in constraint (52). The model is solved again, minimizing the total evacuation time (TET) in the objective function (53). The result is illustrated in Figure 9.

$$Min\ TET = \sum_{k \in K} \sum_{r \in R} \sum_{t \in T} e_r^{kt} \tag{53}$$

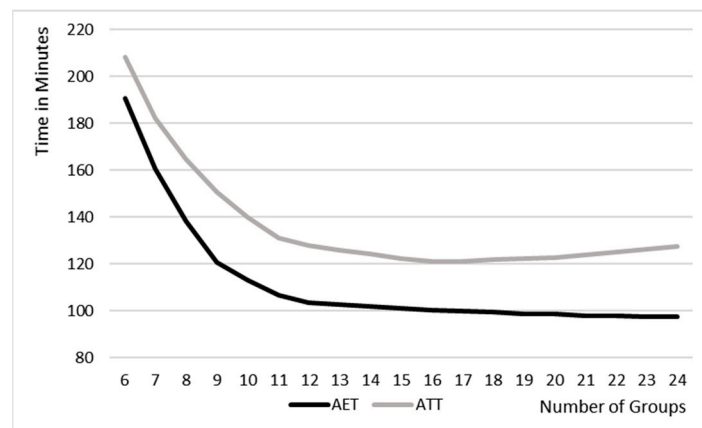


Figure 9. The ATT and AET behavior of 25,000 evacuees when changing the number of groups of evacuees.

subject to

Constraints (31)–(50) and (52)

When a few groups are evacuated, the ATT and AET are high since the number of evacuees in each group is large, leading to higher congestion rates, as illustrated in Figure 9. As the number of groups increases, the ATT and AET decrease. Note that the AET decreases to a point then it increases as the congestion effect fades, and the waiting time to evacuate starts delaying the evacuees. The optimum number of groups to be evacuated depends

on the objective. For the NCT and AET, the number of groups is selected to avoid delays caused by congestion and waiting time, and the number of groups selected in the ATT is the maximum since the waiting time does not affect travel time.

The minimum average travel time is 97.25 when evacuees are grouped into 24 groups, while the minimum average evacuation time is 121.13 when evacuees are grouped into 17 groups.

Assume that the demand to evacuate in the Tampa City network is 45,000 evacuees. Note that the ATT is around 350 min compared to 120 min when 25,000 people are evacuated, and the number of groups is set to nine, as seen in Figure 10. The ATT and AET for the 45,000 evacuees are significantly higher than the 25,000 evacuees since the congestion is higher. Also, the AET for the 45,000 is not considerably affected by the waiting time when the number of groups is set to 24, as shown in Figure 10. From this information, we conclude that all routes can be used for all evacuating times when the demand to evacuate is high in case of emergencies. When all routes are used for all evacuating times, the model becomes LP.

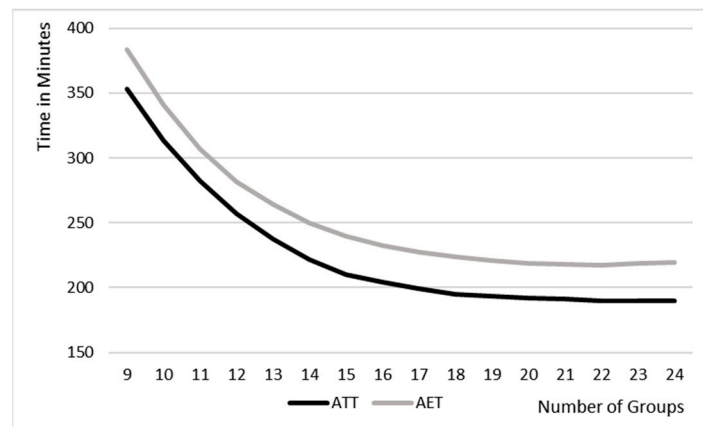


Figure 10. The ATT and AET behavior of 45,000 evacuees when the number of groups is changed.

The number of evacuees in each group is illustrated in Figure 11. Note that the number of evacuees on the routes that cause bottleneck congestion is minimal. The variability in the number of evacuees for the objective NCT is high since the objective is to clear the network in the shortest time. Minimizing the ATT distributes all evacuees on all routes with minimum congestion since the waiting time to be evacuated does not affect the ATT. Note that the number of evacuees does not exceed 2000 vehicles since the delay time for this number of evacuees is insignificant, as seen in Table 3. After 2000, the function becomes steeper, leading to more congestion and delay. Minimizing the AET pushes most evacuees to be evacuated in the early periods to avoid waiting time, as seen in Figure 11.

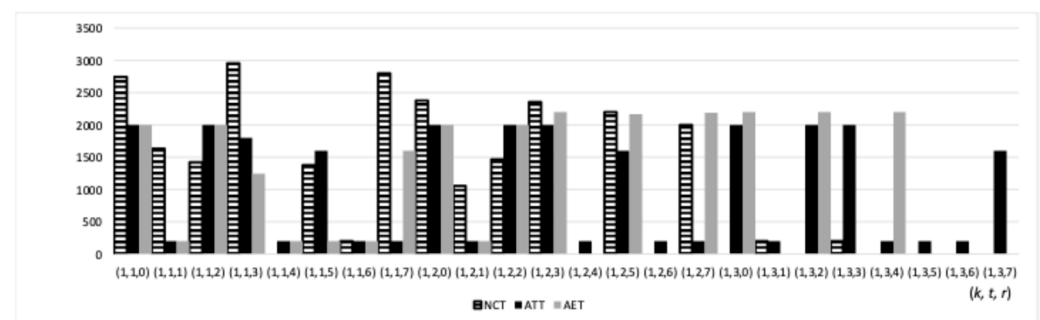


Figure 11. The number of evacuees in each group from community k , on route r , and evacuated at time t .

The travel and evacuation time for each group of evacuees on each route r evacuated at time t for the three objectives is illustrated in Figure 12. Note that the travel time for groups evacuated early is higher due to congestion in the NCT, and the evacuation time is 150 for most groups. The early groups are delayed because of the congestion, while the later groups are delayed waiting to be evacuated. Hence, the model minimized the congestion for the later groups since they were delayed by waiting to evacuate. The variability in the travel time for the ATT is low since all evacuees are distributed on all routes, and evacuating times minimize the overall congestion in the network. The overall travel and evacuation times are minimized for most groups for the AET objective by minimizing the congestion of the network but avoiding waiting time to evacuate.

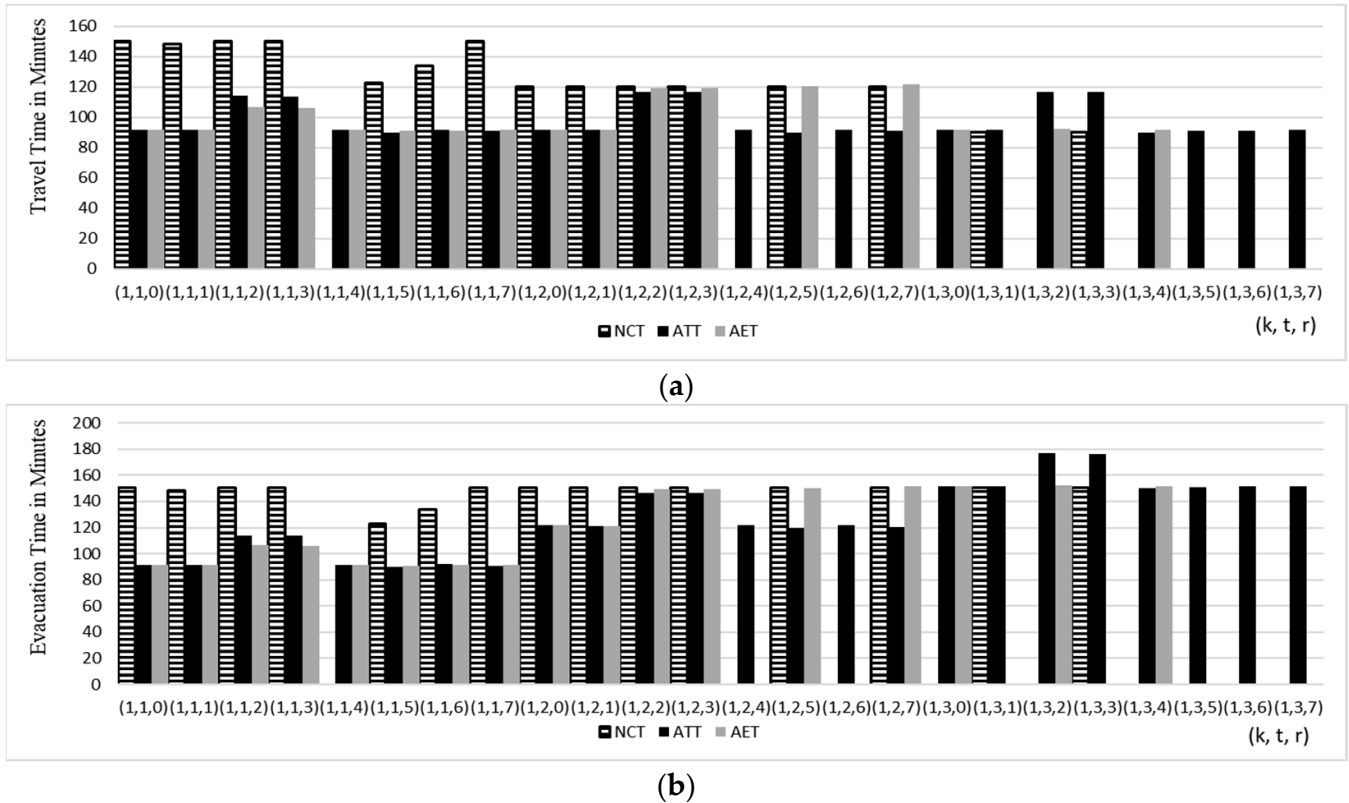


Figure 12. The travel time (a) and evacuation time (b) in minutes for each group of evacuees evacuated on route r at time t .

Comparing the Original LBM Model with the Reduced Complexity Model

The original LBM developed in Section 2 (LBM I) results are compared with the reduced complexity version of the LBM developed in Section 3 (LBM II). The network used is Tampa City with the set of routes $R = \{0, 1, 2, 3, 5, 7\}$. The NCT for LBM I and LBM II is shown in Figure 13 when the demand is from 10,000 to 40,000 evacuees. Note that the NCT is identical in both models; however, the reduction in computational time is significant. The computational times for LBM I and LBM II are illustrated in Figure 14.

Notice that the computational time of the LBM I increases with the demand to evacuate, while the computational time for the LBM II is not affected by the demand. The average computational time for LBM II is 1.25 s. We conclude that the computational time can be reduced by more than 99% while maintaining the same output.

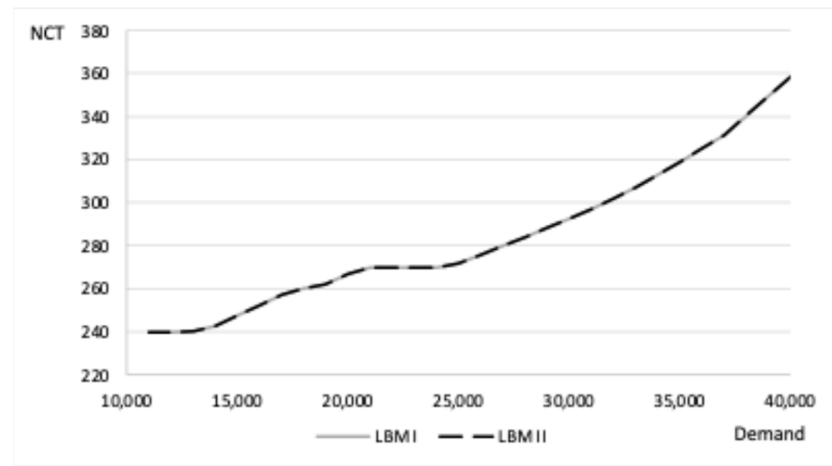


Figure 13. The NCT for the LBM I and LBM II models for demand ranging from 10,000 to 40,000 evacuees.

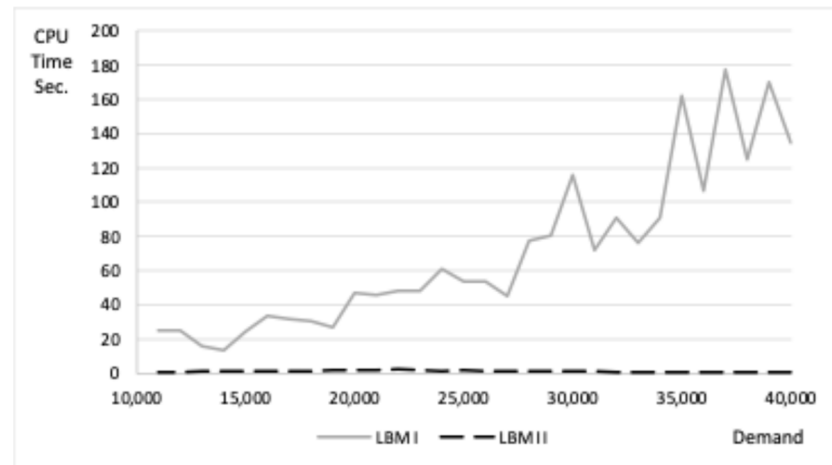


Figure 14. The computational times for the LBM I and LBM II models in seconds when the demand ranges from 10,000 to 40,000 evacuees.

5.3. Computational Complexity

The model is tested on the Tampa City problem using Gurobi Optimizer [46], and the experiment was conducted on a PC with an Intel quad-core 3.4 GH CPU and 32 GB memory. The model can solve small-size problems with a limited number of routes. However, the computational time can increase exponentially with the size of the problem. Note that z_{ijhg}^{ktrv} is the binary variable that indicates the time path of the evacuees. The number of variables z_{ijhg}^{ktrv} used in the model is decided by the number of hubs in a route γ , excluding the terminal hub and the number of routes $|R|$ used in the network. The number of variables z_{ijph}^{kt} in route r is γ^2 at evacuation time $t = 1$. For $t > 1$, the number of variables is $\gamma^2 + (t - 1)\gamma$, and this conclusion leads us to the computational complexity of the model for multiple routes. The computational complexity of the model is $O\left(2^{|R|(\bar{\gamma}^2+(t-1)\bar{\gamma})}\right)$ given that $|R|$ is the number of routes, $\bar{\gamma}$ is the average number of hubs in all routes, excluding the terminal hub, and $t \in T$ is the time of evacuation. The two main factors affecting computational complexity are the number of routes and the average length of these routes.

The computational complexity is significantly reduced in LBM II. The number of variables z_{ijrh}^{kt} used in the model is decided by the number of routes $|R|$ used in the network and the number of evacuating times $|T|$. The number of hubs does not contribute to the number of variables z_{ijrh}^{kt} . The number of variables z_{ijrh}^{kt} in the model is the number of routes r and the number of evacuating times $|T|$. The computational complexity of

the model is reduced from $O\left(2^{|R|(\bar{\gamma}^2+(t-1)\bar{\gamma})}\right)$ to $O\left(2^{|R|\cdot|T|}\right)$ given that $|R|$ is the number of routes. The two main factors affecting computational complexity are the number of routes and evacuating times. However, the computational complexity can be reduced from exponential to polynomial by assuming that all routes are used in all periods of evacuation, as illustrated in Section 4.2. This assumption is valid in the case of emergencies, especially when utilizing all routes since the high demand needs to be evacuated in a short period.

6. Concluding Remarks and Future Works

The latency-based evacuation model reports very detailed information about each group of evacuees, such as their evacuation time, travel time, the route used, latency, and the number of evacuees in each group. However, this information comes at a cost. The computational time increases exponentially with the problem size. The model complexity can be reduced by assuming that all routes are used in all evacuating times. This assumption is valid in the case of high demands to evacuate over a short period of time. The model distributes evacuees on the available routes and evacuating times based on the objective. Minimizing AET is ideal for emergency evacuation and ATT for non-emergencies. When the NCT objective is minimized, the evacuees are randomly distributed on routes as the main objective is to send the evacuees from the endangered zone to the safe destination in the shortest possible time.

In future research, the model's robustness will be tested against the high variability of demands since the demand is uncertain in reality. Since the travel time on each route and evacuating time is estimated in the LBM, fairness among the routes will be implemented to find a balanced solution between the minimum NCT and the minimum evacuation time for each group of evacuees to improve the evacuees' experience in the network.

Author Contributions: Conceptualization, H.B.O.; Methodology, H.B.O. and A.H.; Software, H.B.O., M.M.A. and A.A.; Validation, T.B.T. and M.M.A.; Formal analysis, M.M.A.; Investigation, A.H.; Data curation, H.B.O., A.A. and A.H.; Writing—original draft, H.B.O.; Writing—review & editing, H.B.O.; Supervision, T.B.T.; Project administration, T.B.T. All authors have read and agreed to the published version of the manuscript.

Funding: This research received no external funding.

Data Availability Statement: The data presented in this study are available on request from the corresponding author.

Acknowledgments: The authors gratefully acknowledge the funding of the Deanship of Graduate Studies and Scientific Research, Jazan University, Saudi Arabia, through Project Number GSSRD-24.

Conflicts of Interest: The authors declare no conflicts of interest.

References

1. Bish, D.R.; Sherali, H.D.; Hobeika, A.G. Optimal Evacuation Planning Using Staging and Routing. *J. Oper. Res. Soc.* **2014**, *65*, 124–140. [[CrossRef](#)]
2. Duan, X.H.; Wu, J.X.; Xiong, Y.L. Dynamic emergency vehicle path planning and traffic evacuation based on salp swarm algorithm. *J. Adv. Transp.* **2022**, *2022*, 7862746. [[CrossRef](#)]
3. Mtoi, E.T.; Moses, R. Calibration and evaluation of link congestion functions. *J. Transp. Technol.* **2014**, *4*. [[CrossRef](#)]
4. Daganzo, C.F. The cell transmission model: A dynamic representation of highway traffic consistent with the hydrodynamic theory. *Transp. Res. Part B Methodol.* **1994**, *28*, 269–287. [[CrossRef](#)]
5. Daganzo, C.F. The cell transmission model, part II: Network traffic. *Transp. Res. Part B Methodol.* **1995**, *29*, 79–93. [[CrossRef](#)]
6. Ziliaskopoulos, A.K. A linear programming model for the single destination system optimum dynamic traffic assignment problem. *Transp. Sci.* **2000**, *34*, 37–49. [[CrossRef](#)]
7. Jahn, O.; Möhring, R.H.; Schulz, A.S.; Stier-Moses, N.E. System-optimal routing of traffic flows with user constraints in networks with congestion. *Oper. Res.* **2005**, *53*, 600–616. [[CrossRef](#)]

8. Janson, B.N. Dynamic traffic assignment for urban road networks. *Transp. Res. Part B Methodol.* **1991**, *25*, 143–161. [[CrossRef](#)]
9. Jayakrishnan, R.; Tsai, W.K.; Chen, A. A dynamic traffic assignment model with traffic-flow relationships. *Transp. Res. Part C Emerg. Technol.* **1995**, *3*, 51–72. [[CrossRef](#)]
10. Kachroo, P.; Sastry, S. Traffic assignment using a density-based travel-time function for intelligent transportation systems. *IEEE Trans. Intell. Transp. Syst.* **2016**, *17*, 1438–1447. [[CrossRef](#)]
11. Kaufman, D.E.; Nonis, J.; Smith, R.L. A mixed integer linear programming model for dynamic route guidance. *Transp. Res. Part B Methodol.* **1998**, *32*, 431–440. [[CrossRef](#)]
12. Wie, B.W.; Friesz, T.L.; Tobin, R.L. Dynamic user optimal traffic assignment on congested multideestination networks. *Transp. Res. Part B Methodol.* **1990**, *24*, 431–442. [[CrossRef](#)]
13. Wardrop, J.G. Some theoretical aspects of road traffic research. *Inst. Civil. Eng. Proc.* **1952**, *1*, 325–362. [[CrossRef](#)]
14. Friesz, T.L.; Bernstein, D.; Smith, T.E.; Tobin, R.L.; Wie, B.W. A variational inequality formulation of the dynamic network user equilibrium problem. *Oper. Res.* **1993**, *41*, 179–191. [[CrossRef](#)]
15. Smith, M.J. A new dynamic traffic model and the existence and calculation of dynamic user equilibria on congested capacity-constrained road networks. *Transp. Res. Part B Methodol.* **1993**, *27*, 49–63. [[CrossRef](#)]
16. Southworth, F. *Regional Evacuation Modeling: A State of the Art Reviewing*; (No. ORNL/TM-11740); ORNL Oak Ridge National Laboratory (US): Oak Ridge, TN, USA, 1991.
17. Correa, J.R.; Schulz, A.S.; Stier-Moses, N.E. Fast, fair, and efficient flows in networks. *Oper. Res.* **2007**, *55*, 215–225. [[CrossRef](#)]
18. Merchant, D.K.; Nemhauser, G.L. A model and an algorithm for the dynamic traffic assignment problems. *Transp. Sci.* **1978**, *12*, 183–199. [[CrossRef](#)]
19. Merchant, D.K.; Nemhauser, G.L. Optimality conditions for a dynamic traffic assignment model. *Transp. Sci.* **1978**, *12*, 200–207. [[CrossRef](#)]
20. Carey, M. A constraint qualification for a dynamic traffic assignment model. *Transp. Sci.* **1986**, *20*, 55–58. [[CrossRef](#)]
21. Wie, B.W.; Tobin, R.L.; Friesz, T.L.; Bernstein, D. A discrete time, nested cost operator approach to the dynamic network user equilibrium problem. *Transp. Sci.* **1995**, *29*, 79–92. [[CrossRef](#)]
22. Carey, M.; McCartney, M. Behaviour of a whole-link travel time model used in dynamic traffic assignment. *Transp. Res. Part B Methodol.* **2002**, *36*, 83–95. [[CrossRef](#)]
23. Carey, M. Nonconvexity of the dynamic traffic assignment problem. *Transp. Res. Part B Methodol.* **1992**, *26*, 127–133. [[CrossRef](#)]
24. Carey, M.; Subrahmanian, E. An approach to modelling time-varying flows on congested networks. *Transp. Res. Part B Methodol.* **2000**, *34*, 157–183. [[CrossRef](#)]
25. Drissi-Kaitouni, O.; Hamed-Benchekroun, A. A dynamic traffic assignment model and a solution algorithm. *Transp. Sci.* **1992**, *26*, 119–128. [[CrossRef](#)]
26. Li, J.; Fujiwara, O.; Kawakami, S. A reactive dynamic user equilibrium model in network with queues. *Transp. Res. Part B Methodol.* **2000**, *34*, 605–624. [[CrossRef](#)]
27. Lighthill, M.J.; Whitham, G.B. On kinematic waves I. Flood movement in long rivers. *Proc. R. Soc. London. Ser. A. Math. Phys. Sci.* **1955**, *229*, 281–316.
28. Richards, P.I. Shock waves on the highway. *Oper. Res.* **1956**, *4*, 42–51. [[CrossRef](#)]
29. Ukkusuri, S.V.; Waller, S.T. Linear programming models for the user and system optimal dynamic network design problem: Formulations, comparisons and extensions. *Netw. Spat. Econ.* **2008**, *8*, 383–406. [[CrossRef](#)]
30. Nie, Y.M. A cell-based Merchant–Nemhauser model for the system optimum dynamic traffic assignment problem. *Transp. Res. Part B Methodol.* **2011**, *45*, 329–342. [[CrossRef](#)]
31. Anshelevich, E.; Ukkusuri, S. Equilibria in dynamic selfish routing. In *International Symposium on Algorithmic Game Theory*; Springer: Berlin/Heidelberg, Germany, 2009; pp. 171–182.
32. Hayrapetyan, A.; Tardos, É.; Wexler, T. A network pricing game for selfish traffic. *Distrib. Comput.* **2007**, *19*, 255–266. [[CrossRef](#)]
33. Nikolova, E.; Stier-Moses, N.E. Stochastic selfish routing. In *International Symposium on Algorithmic Game Theory*; Springer: Berlin/Heidelberg, Germany, 2011; pp. 314–325.
34. Van Essen, M.; Thomas, T.; van Berkum, E.; Chorus, C. From user equilibrium to system optimum: A literature review on the role of travel information, bounded rationality and non-selfish behaviour at the network and individual levels. *Transp. Rev.* **2016**, *36*, 527–548. [[CrossRef](#)]
35. Shirke, C.; Bhaskar, A.; Chung, E. Macroscopic modelling of arterial traffic: An extension to the cell transmission model. *Transp. Res. Part C Emerg. Technol.* **2019**, *105*, 54–80. [[CrossRef](#)]
36. Wu, Y.; Lin, Y.; Hu, R.; Wang, Z.; Zhao, B.; Yao, Z. Modeling and simulation of traffic congestion for mixed traffic flow with connected automated vehicles: A cell transmission model approach. *J. Adv. Transp.* **2022**, *2022*, 8348726. [[CrossRef](#)]
37. Alimardani, F.; Baras, J.S. PWA-CTM: An Extended Cell-Transmission Model based on Piecewise Affine Approximation of the Fundamental Diagram. In *Proceedings of the 2022 30th Mediterranean Conference on Control and Automation (MED)*, Vouliagmeni, Greece, 28 June–1 July 2022; IEEE: New York, NY, USA, 2002; pp. 1059–1065.

38. Bayram, V.; Yaman, H. A Joint Demand and Supply Management Approach to Large Scale Urban Evacuation Planning: Evacuate or Shelter-in-Place, Staging and Dynamic Resource Allocation. *Eur. J. Oper. Res.* **2023**, *313*, 171–191. [[CrossRef](#)]
39. Tang, K.; Osaragi, T. Multi-Objective Evacuation Planning Model Considering Post-Earthquake Fire Spread: A Tokyo Case Study. *Sustainability* **2024**, *16*, 3989. [[CrossRef](#)]
40. Liperda, R.I.; Putra, R.P.; Pairunan, G.B.; Maghfiroh, M.F.N.; Redi, A.A.N.P. Comparative Analysis of Electric and Conventional Vehicles Performance in the Evacuation Process of Mount Semeru Eruption Victims Based on Geographic Information Systems. *Sustainability* **2024**, *16*, 8939. [[CrossRef](#)]
41. Insani, N.; Taheri, S.; Abdollahian, M. A Mathematical Model for Integrated Disaster Relief Operations in Early-Stage Flood Scenarios. *Mathematics* **2024**, *12*, 1978. [[CrossRef](#)]
42. Lu, F.; Du, Z.; Wang, Z.; Wang, L.; Wang, S. Towards Enhancing the Crowdsourcing Door-To-Door Delivery: An Effective Model in Beijing. *J. Ind. Manag. Optim.* **2024**, *21*, 2371–2395. [[CrossRef](#)]
43. Khalili, S.M.; Mojtahedi, M.; Steinmetz-Weiss, C.; Sanderson, D. A Systematic Literature Review on Transit-Based Evacuation Planning in Emergency Logistics Management: Optimisation and Modelling Approaches. *Buildings* **2024**, *14*, 176. [[CrossRef](#)]
44. Krutein, K.F.; Goodchild, A. The Isolated Community Evacuation Problem with Mixed Integer Programming. *Transp. Res. Part E Logist. Transp. Rev.* **2022**, *161*, 102710. [[CrossRef](#)]
45. Flores, I.; Ortuño, M.T.; Tirado, G. A Goal Programming Model for Early Evacuation of Vulnerable People and Relief Distribution during a Wildfire. *Saf. Sci.* **2023**, *164*, 106117. [[CrossRef](#)]
46. Gurobi Optimization, LLC. *Gurobi Optimizer*, Version 9.5.; Gurobi Optimization, LLC: Beaverton, OR, USA, 2023.

Disclaimer/Publisher’s Note: The statements, opinions and data contained in all publications are solely those of the individual author(s) and contributor(s) and not of MDPI and/or the editor(s). MDPI and/or the editor(s) disclaim responsibility for any injury to people or property resulting from any ideas, methods, instructions or products referred to in the content.